JOURNAL OF Materials CHEMISTRY

# Structural evolution and associated properties on conversion from Si-C-O-Al ceramic fibers to Si-C-Al fibers by sintering

**Feng Cao,[b]† Xiao-dong Li,[b] Ping Peng,[b] Chung-xiang Feng,[b] Jun Wang[b] and Dong-pyo Kim*[a]**

[a]*Department of Fine Chemicals Engineering and Chemistry, Chungnam National University, Taejon 305-764, Korea. E-mail: dpkim@cnu.ac.kr; Fax: 82-42-823-6665*
[b]*Key Laboratory of Ceramic Fibers and Composites, National University of Defense Technology, Changsha 410073, P.R. China*

***Received 30th July 2001, Accepted 3rd December 2001***
***First published as an Advance Article on the web 4th February 2002***

Ceramic fibers with the Si-C-O-Al composition were prepared by melt-spinning of polyaluminocarbosilane (PACS), initial curing in air and then thermal curing, before finally being pyrolyzed at 1300 °C. The ceramic fibers so-obtained were sintered at 1800 °C in argon to produce Si-C-Al ceramic fibers as a super high temperature-resistant reinforcement. When the Si-C-O-Al fibers were sintered to the Si-C-Al ceramic fibers, the structural evolution and the associated properties were studied in comparison to PCS-derived Si-C-O ceramic fibers with respect to tensile strength, creep resistance, electrical resistivity, morphology, and crystalline grain size using $^{29}$Si MAS NMR, $^{13}$C MAS NMR, AES, XRD and SEM. The Si-C-O-Al ceramic fibers had low creep resistance because they contained high levels of silicon oxycarbide, poorly organized SiC crystalline grains at the nanometer level and high levels of free carbon. The electrical resistivity of the Si-C-O-Al ceramic fibers was high due to the high level of silicon oxycarbide. However, the Si-C-Al ceramic fibers were strongly resistant to creep due to a silicon oxycarbide free structure, a well-organized and crystallized SiC content and a lower content of free carbon. The absence of silicon oxycarbide in the Si-C-Al ceramic fibers is responsible for their low electrical resistivity and high tensile strength retention at high temperature.

## Introduction

As a typical candidate for non-oxide ceramic fibers, SiC fibers derived from polyorganosilane have been widely studied over the past two decades, and this has resulted in commercially available Nicalon and Tyranno products, which are used to manufacture high performance ceramic matrix composites (CMCs).[1–3] Attempts have been made to overcome the drawbacks of Nicalon grade fibers, *i.e.* degradation at high temperature, and this has resulted in the development of a series of SiC fibers which are stable at high temperatures, known as Hi-Nicalon-S (Nippon Carbon) and Sylramic (Dow-Corning).[1–3] In particular, Ube Industries[4,5] manufacture a super high temperature-resistant Si-C-Al fiber (commercial name Tyranno SA), which is produced by sintering Si-C-O-Al fibers at 1800 °C, after a preparation that involves air curing and pyrolysis at 1300 °C of a spun polyaluminocarbosilane (PACS) feedstock.

The microstructure of such sintered fibers and their ceramic matrix composites have been studied.[3–6] However, the evolution of the microstructure and the associated property changes which occur during sintering have not been systematically clarified. In this study, we focus on the relationship between the properties and structures of Si-C-O-Al ceramic fibers during their transformation to Si-C-Al fibers by the high temperature sintering process. Furthermore, we report a simplified manufacturing procedure, including details of a synthetic route which involves the synthesis of the precursor at atmospheric pressure without an autoclave.

## Experimental

### Preparation of ceramic fibers

Si-C-O-Al and Si-C-Al ceramic fibers were prepared by a modification of the procedure of Ishikawa *et al.*[4] Polyaluminocarbosilane (PACS) as a precursor of the Si-C-O-Al and Si-C-Al ceramic fibers was synthesized by thermolysis of a mixture of 15 g polysilacarbosilane (PSCS) and 2 g aluminum acetylacetonate [$(AcAc)_3Al$; Aldrich, 99%) above 300 °C in $N_2$ at atmospheric pressure. PSCS having Si–$CH_2$-Si and Si–Si linkages in the backbone, with number average molecular weight 1120, was readily prepared by partial conversion of polydimethylsilane (PDMS), purchased from Xinhuo Company, at 400 °C under $N_2$. The PACS so obtained was resolved in xylene, filtered and vacuum distilled to remove insoluble species and oligomer. The gold-colored solid PACS obtained had a number average molecular weight of ~1500 and a softening point of 250 °C, and was melt-spun into continuous fibers. The green fibers were cured at 170–190 °C in air for 2–3.5 h and then transferred to a sealed quartz furnace in an $N_2$ atmosphere to be thermally cured at a temperature increment of 1 °C min$^{-1}$ to 450 °C for 2 h. The cured fiber was then pyrolyzed at 1300 °C for 1 h to produce the Si-C-O-Al ceramic fibers, and these were further sintered at 1800 °C for 1 h in argon to produce the Si-C-Al ceramic fibers. For comparison purposes, PSCS without aluminum acetylacetonate was thermolysized into polycarbosilane (PCS) under the same condition as applied for preparation of the PACS and then spun into fibers, air-cured at 170–190 °C for 5–10 h, and finally pyrolyzed at 1300 °C for 1 h to provide Si-C-O ceramic fibers.

### Thermal treatment of ceramic fibers and characterization

To investigate the effect of the heat treatment on their tensile strengths and the electrical properties, the Si-C-O-Al, Si-C-Al and Si-C-O ceramic fibers were thermally exposed to various heat treatment temperatures (1000, 1200, 1400, 1600, and 1800 °C) in argon for 1 h. Tensile strength was measured using single filaments of length 25 mm at room temperature. Every data point is the average value of 25 monofilaments. Measurements of electrical resistivity were performed using the standard four-point method.[7,8] Single fibers were connected to four minute copper contacts; the two external contacts were employed to

†Worked at Prof. Kim's Lab. under the co-advisor system.

 DOI: 10.1039/b106868g

**This journal is © The Royal Society of Chemistry 2002**

apply current and the inner two to measure the corresponding potential. Fiber diameter was determined using a microscope.

The creep resistance of the ceramic fibers was determined using the bend stress relaxation (BSR) method of Dicarlo.[9] In this method, ceramic fibers were wound around a graphite rod of radius $R_0$ (8 mm) and put it in a programmable furnace, set at different pre-selected temperatures (800, 1000, 1200, 1400, 1600 and 1800 °C) which were aattained at a rate of 50 °C $min^{-1}$, and the maximum temperatures reached were held for 1 h in Ar. The stress relation ratio, $m$, was determined using the radius, $R$, of the relaxed fibers at room temperature from the following equation:

$$m = 1 - (R_0/R)$$

The value of $m$ is therefore lies in the range 0–1, and the higher the $m$ value, the better is the creep resistance of the fiber.

The X-ray diffraction patterns (Siemens D5000, Cu-K$\alpha$ radiation, $\lambda = 0.154$ nm) were obtained from powdered fiber. The apparent mean grain size, $L$, of the SiC crystalline phase was calculated from the width, $D$ (in radians), of the (111) diffraction peak at mid-height, according to the Scherrer equation:

$$L = K\lambda/D\cos\theta$$

Fiber morphology was studied by scanning electron microscopy (SEM, JEOL JSM-6300). Ceramic fibers were milled into fine powders for solid-state nuclear magnetic resonance (NMR) analysis using a 400 MHz Bruker DSX400 pectrometer, which was calibrated with tetramethylsilane (TMS) for $^{29}$Si NMR at 0ppm and adamatane for $^{13}$C NMR at 38.3 ppm. The samples were spun at 4000–5000 Hz, according to the magic-angle spinning (MAS) technique. Auger electron spectroscopy (AES) was performed with a scanning microprobe (VG MICROLAB 310D) equipped with an $Ar^+$ sputtering gun (etching conditions: 5 Kev, 600 nA; etching rate: 2.5 Å $sec^{-1}$; angle: 0°), which allowed point analyses (analysis area: 3500 Å × 3500 Å) to be made at the fiber surface at an electron beam voltage of 10 KeV. The densities of ceramic fibers were measured at room temperature by the sink–float method using various mixtures of carbon tetrachloride ($CCl_4$, density 1.6 g $ml^{-1}$) and methylene iodide ($CH_2I_2$, density 3.3 g $ml^{-1}$). Elemental analysis of bulk ceramic fibers for Si, C, O and Al content was performed at the Zhongnan Institute of Metallurgy. For the measurement of Si content, a ceramic fiber sample was attacked by a fused alkali salt followed by neutralization with hydrochloric acid. Silicon content was determined by gravimetry of $SiO_2$ obtained from above solution. In order to measure Al content, a ceramic fiber sample was decomposed by means of fused sodium hydroxide and then neutralized with an acid for spectrophotometry. Carbon content was established by using IR spectroscopy to measure the carbon dioxide released on burning a sample at high temperature in oxygen. The measurement of oxygen content in SiC fibers was carried out using equivalent analysis (oxygen meter, IRO-1, Shanghai YQFX Co. Ltd.). A sample was charged in a graphite container and the temperature raised to 3000 °C as quickly as possible to turn oxygen in the sample into CO, the amount of CO produced was subsequently measured with a CO meter.

## Results and discussion

In this study, three types of ceramic fibers were prepared under different conditions, Si-C-O-Al fibers and Si-C-Al fibers were obtained from the same PACS, and these were compared to Si-C-O fibers obtained by pyrolysis of PCS fibers at 1300 °C for 1 h. The precursor PACS used for the Si-C-O-Al and Si-C-Al ceramic fibers and the precursor PCS for the Si-C-O ceramic fibers were synthesized under atmospheric pressure, which has clear manufacturing cost implications.

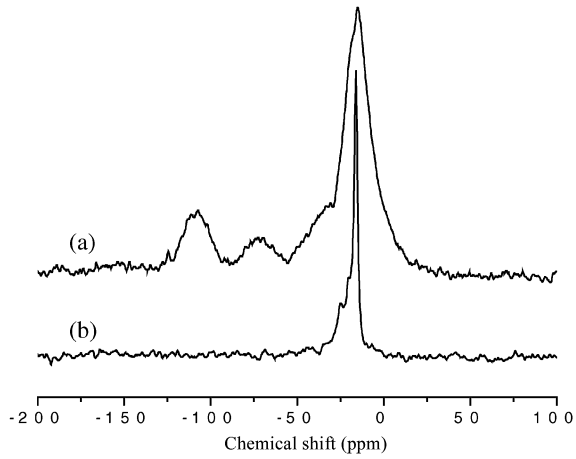


**Fig. 1** $^{29}$Si MAS NMR spectra of (a) Si-C-O-Al and (b) Si-C-Al fibers.

The $^{29}$Si MAS NMR spectra shown in Fig. 1 demonstrate the structural evolution after sintering. In Fig. 1(a), the resonance peak centered at −14.7 ppm and the shoulder at around −18.7 ppm, are assigned to ordered and disordered β-SiC,[10] respectively. In addition, the $SiC_3O$ resonance ($\approx$0 ppm) is believed to be hidden by the broad peak at −14.7 ppm in the spectrum of the Si-C-O-Al fibers;[11] the resonance peaks at −32, −72 and −107 ppm are assigned to the $SiC_2O_2$, $SiCO_3$, and $SiO_4$ phases, respectively.[10–13] In Fig. 1(b), the peaks at −15.9, −19.9, and −24.7 ppm are assigned to ordered β-SiC, disordered β-SiC, and α-SiC,[10] respectively. By comparing the two spectra, three aspects of the structural evolution of Si-C-O-Al ceramic fibers are implied: firstly, the $SiC_xO_y$ and $SiO_4$ phases in the Si-C-O-Al ceramic fibers are removed by sintering, since there are no corresponding peaks in the spectrum of the Si-C-Al ceramic fibers, secondly, the percentage of ordered β-SiC increases after sintering, since the peak assigned to disordered β-SiC in the Si-C-Al fibers is much smaller after sintering, and the last aspect is the slight upfield chemical shift of ordered β-SiC (from −14.7 to −15.9 ppm) after sintering. The upfield chemical shift is presumably caused by a deprotonation reaction occurring at the C sites with Si sites.[14] The shift could also be related to an ordering of the various sites. In addition, a small amount of α-SiC was detected after sintering.

Fig. 2 shows the $^{13}$C MAS NMR spectra of Si-C-O-Al fibers and Si-C-Al fibers. Both show two main peaks centered around 22–24 ppm and 127 ppm, which are mainly assigned to the $CSi_4$ tetrahedral structure (C $sp^3$) of β-SiC and the graphite-like

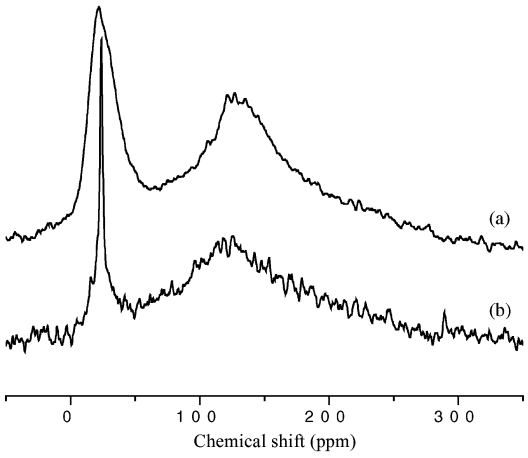


**Fig. 2** $^{13}$C MAS NMR spectra of (a) Si-C-O-Al and (b) Si-C-Al fibers.

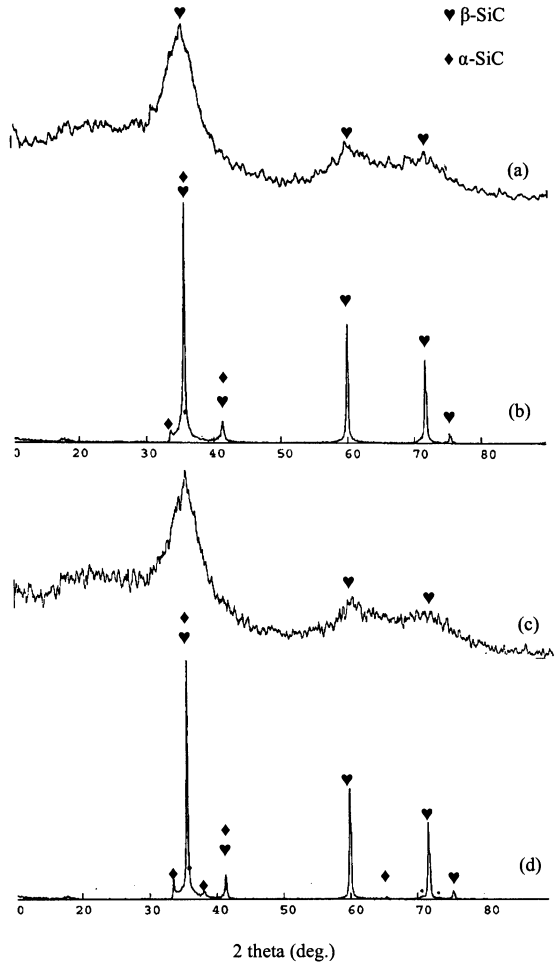


**Fig. 3** XRD patterns of (a) Si-C-O-Al fibers, (b) Si-C-Al fibers, (c) Si-C-O fibers and (d) Si-C-O fibers sintered at 1800 °C in Ar for 30 min.

polyaromatic structure (C $sp^2$),[15–17] respectively. After sintering the Si-C-O-Al fibers at 1800 °C, the shoulder centered around 29.7 ppm [Fig. 2(a)] which is assigned to the $SiC_xO_y$ phase;[11] disappears. Furthermore, another weak shoulder centered at 15.6 ppm, which is assigned to α-SiC, becomes weaker, which is consistent with the above $^{29}$Si MAS NMR data.[16] The linewidth of the peak assigned to β-SiC in the Si-C-Al fibers is much narrower than that of the Si-C-O-Al fibers, suggesting better organized β-SiC in the Si-C-Al fibers. The relative intensity of the broad peak centered around 127 ppm for the Si-C-O-Al fibers is obviously higher than that of the Si-C-Al fibers, which indicates a lower free carbon content in the Si-C-Al ceramic fibers compared to the Si-C-O-Al ceramic fibers.

XRD patterns (Fig. 3) indicate that the SiC crystal grain size in the Si-C-O ceramic fibers grows from 2 nm at 1300 °C to 105 nm at 1800 °C; for Si-C-O-Al fibers, the growth of the SiC crystal grain size is a little slower than that of Si-C-O ceramic fibers (from 2 nm at 1300 °C to 95 nm at 1800 °C), which was probably due to hetero-elemental Al and the lower oxygen content, which in the ceramic fibers means a lower level of silicon oxycarbide that can be consumed at high temperature to form coarsened SiC.[11] Both the Si-C-Al fibers and sintered Si-C-O fibers contain a small amount of α-SiC in addition to β-SiC. This is consistent with the NMR results for the Si-C-Al fibers, which show two peaks (−24.7 ppm in the $^{29}$Si MAS NMR and 15.6 ppm in the $^{13}$C MAS NMR) assigned to α-SiC. Furthermore, the percentage of α-SiC in the sintered Si-C-O fibers seems higher than that in the Si-C-Al fibers with respect to their relative intensities by XRD.

Auger electron spectroscopy (AES), shown Fig. 4, suggests an elemental composition (Si, C, O and Al) as relative

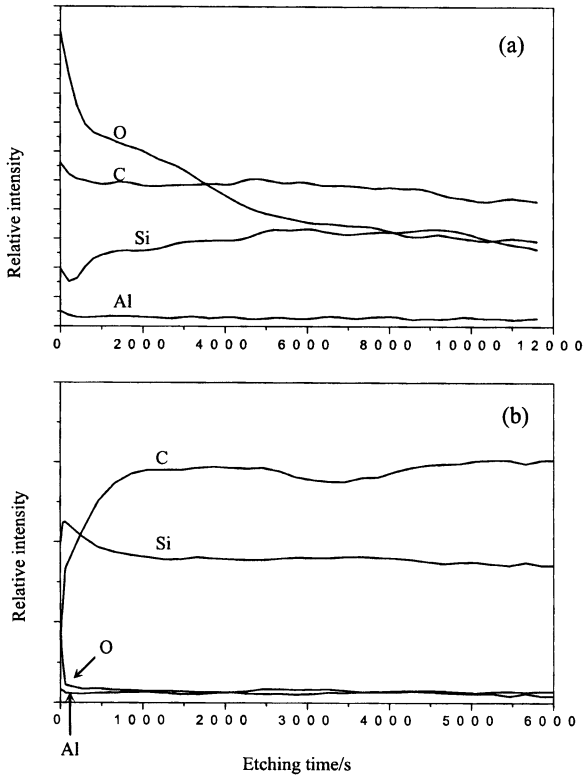


**Fig. 4** AES depth profiles of (a) Si-C-O-Al and (b) Si-C-Al fibers (sputtering rate:15 nm $min^{-1}$).

percentages, which could be derived from the measured relative intensities. It is immediately evident that the percentage of oxygen in the Si-C-Al fibers is much lower than that in the Si-C-O-Al fibers, which is in good agreement with the above $^{29}$Si MAS NMR results. The Si-C-Al ceramic fibers are still rich in carbon, which is consistent with the $^{13}$C MAS NMR spectrum showing a broad peak around 127 ppm. The distribution of oxygen in both the Si-C-O-Al and Si-C-Al fibers is indicative of the presence of an oxygen-enriched layer (≈25 nm for the Si-C-Al fibers; ≈125 nm for the Si-C-O-Al fibers). Table 1 shows the evolution of the chemical composition of ceramic fibers during sintering at 1800 °C. The Si-C-O-Al fibers are rich in carbon (C/Si in atom, 1.51), contain 9.85 wt.% oxygen and 0.68 wt.% aluminum. After sintering at 1800 °C, the oxygen content and the C/Si ratio decrease obviously, which is consistent with the AES and NMR results. The aluminum content is slightly increased due to the removal of some oxygen and free carbon. Comparatively, the oxygen content of the Si-C-O fibers is higher than that of the Si-C-O-Al fibers due to the longer air-curing time. After sintering at 1800 °C, most of the oxygen and free carbon in the Si-C-O fibers is also removed, resulting in near-stoichiometric SiC with severe degradation of the mechanical properties.

Fig. 5 shows SEM surface micrographs of ceramic fibers. The Si-C-O fibers sintered at 1800 °C without Al have an extremely rough surface on which many particles of about 0.5 μm in size, presumably crystalline SiC, grow excessively during the heat treatment.[18] However, the Si-C-O-Al fibers have a very

**Table 1** Elemental analyses of the various ceramic fibers

| Type of fiber (final heating temp./°C) | C/ wt.% | Si/ wt.% | C/Si (atom) | O/ wt.% | Al/ wt.% |
|---|---|---|---|---|---|
| Si-C-O-Al (1300) | 35.19 | 54.52 | 1.51 | 9.58 | 0.68 |
| Si-C-Al (1800) | 32.43 | 65.70 | 1.15 | 0.98 | 0.84 |
| Si-C-O (1300) | 33.77 | 52.65 | 1.49 | 13.76 | 0 |
| Si-C-O (1800) | 30.95 | 68.28 | 1.06 | 0.85 | 0 |

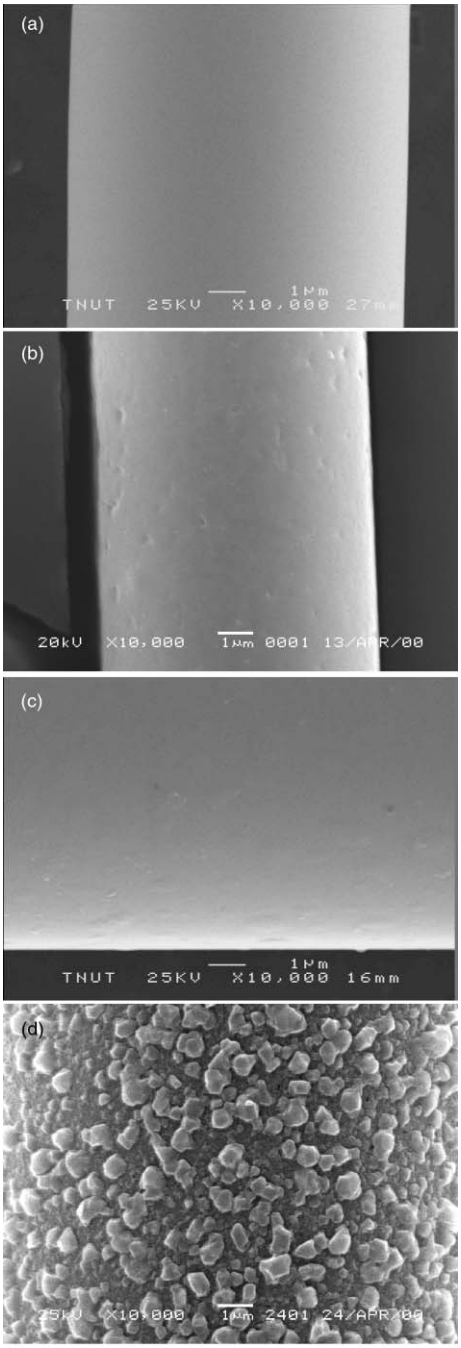


**Fig. 5** SEM micrographs of (a) Si-C-O-Al fibers, (b) Si-C-Al fibers, (c) Si-C-O fibers and (d) Si-C-O fibers sintered at 1800 °C in Ar for 1 h.

smooth surface without any observable flaws. Furthermore, after sintering at 1800 °C, the Si-C-O-Al fibers shrink by a remarkable 18% from 10 to 8.2 μm in average diameter, while the Si-C-O fibers average diameter changes only by 14.3% from 14 to 12 μm. The higher shrinkage of the Si-C-O-Al fibers indicates a higher level of densification, and suggests that pores and defects formed by the removal of oxygen and excess carbon might be efficiently healed by sintering in the presence of Al.[4] This is also consistent with other reports which describe the use of $Al_2O_3$ as a sintering aid.[19–21] Furthermore, the density evolution of ceramic fibers during sintering is also consistent, as shown in Table 2. Initially, there is not much difference between the densities of Si-C-O-Al fiber and Si-C-O fibers. After sintering at 1800 °C, the density of the Si-C-Al fibers increases significantly to 3.07 g $cm^{-3}$ due to densification resulting from the sintering behavior of Al and removal of free carbon and the $SiC_xO_y$ phase. Conversely, the density of the Si-C-O fibers decreases to 2.38 g $cm^{-3}$.

**Table 2** Density evolution of ceramic fibers

| Ceramic fibers | Si-C-O-Al fibers | Si-C-Al fibers | Si-C-O fibers | Si-C-O fibers sintered at 1800 °C |
|---|---|---|---|---|
| Density/g $cm^{-3}$ | 2.53 | 3.07 | 2.51 | 2.38 |

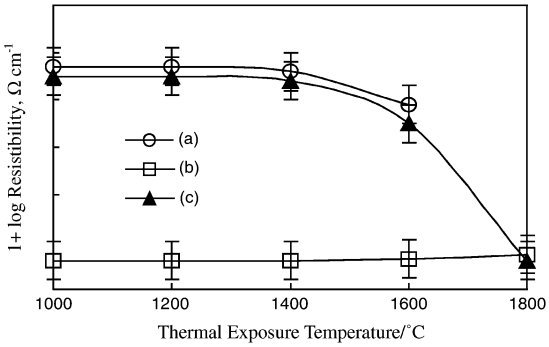


**Fig. 6** Room temperature electrical resistivities of (a) Si-C-O-Al, (b) Si-C-Al and (c) Si-C-O fibers, all after 1 h thermal exposure to various temperatures in argon.

Fig. 6 shows the room temperature electrical resistivity of ceramic fibers as a function of the thermal exposure temperature. The as-obtained Si-C-O-Al and Si-C-O fibers show high resistivity, which decreases rapidly after treatment at over 1600 °C and finally exhibit a resistivity of 0.4 ohm $cm^{-1}$ at 1800 °C. The electrical resistivity of the Si-C-O fibers is a little higher than that of the Si-C-O-Al fibers, because the former were cured in air for a longer period and consequently have higher oxygen content than the latter. The electrical resistivity of the Si-C-Al fibers is much lower than that of either the Si-C-O-Al or the Si-C-O fibers, and slightly increases on heating to 1600 °C. Their higher electrical conductivity may be related to their much lower oxygen content and low percentage of free carbon. Narisawa *et al.*[22] confirmed that a reduction in oxygen content in polymer-derived fibers reduces the resistivity so that near-stoichiometric fibers have a rather low resistivity. In fact, the electrical resistivity of stoichiometric SiC is as high as $1 \times 10^6$ ohm $cm^{-1}$.[23] A small percentage of free C is likely to be responsible for the conductivity of the Si-C-Al fibers. Our results are consistent with the reports of other researchers on this topic.[24]

Fig. 7 shows the room temperature tensile strength as a function of thermal treatment temperature. The tensile strength of the Si-C-O-Al fibers slowly reduces after exposure to high temperatures, for example, after thermal exposure at 1800 °C in argon, 78% of the initial tensile strength was preserved. In contrast, PCS-derived Si-C-O ceramic fibers begin to degrade

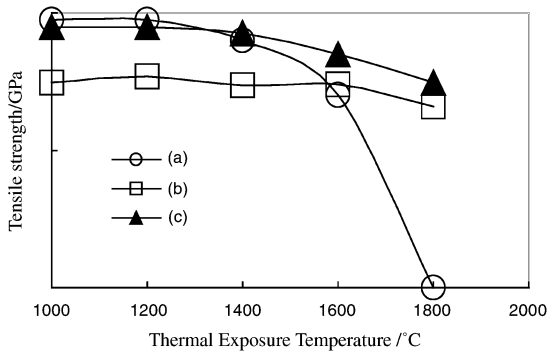


**Fig. 7** Room temperature tensile strengths of (a) Si-C-O, (b) Si-C-Al and (c) Si-C-O-Al fibers, all after 1 h thermal exposure to various temperatures in argon.

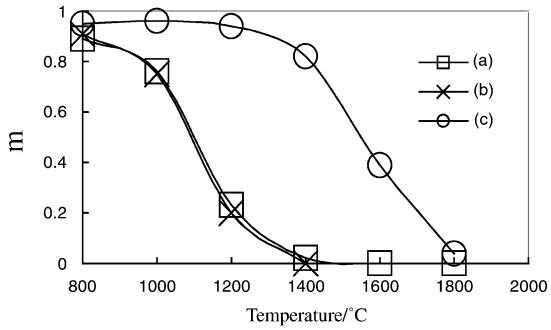


**Fig. 8** One hour bend–stress relaxation ratios of (a) Si-C-O-Al, (b) Si-C-O and (c) Si-C-Al fibers, as function of temperature, all in argon.

in strength dramatically at temperatures over 1400 °C, and have little strength at 1800 °C. The higher tensile strength retention of Si-C-O-Al fibers after sintering at 1800 °C is presumably attributable to two reasons. The first is associated with the incorporated Al, which may play a role as a sintering aid to densify the fibers at high temperatures, as observed by SEM.[4] Secondly, PACS green fibers are consolidated by the combination of brief air-curing and further thermal curing in an inert atmosphere to minimize the oxygen content of the ceramic fibers; while the PCS green fibers were cured only in air for an extended period, which incorporates a lot of oxygen into the green fibers, forming Si-C-O fibers. Furthermore, the produced silicon oxycarbide phase must be decomposed into volatile CO and SiO at high temperatures, which results in the tensile strength degradation.[11] The reduction in the Si-C-O-Al fiber tensile strength observed after sintering at 1800 °C is likely caused by crystal coarseness; while the tensile strength reduction of the Si-C-O fibers is attributed to a combination of SiC grain coarsening and flaw formation, such as that due to the creation of pores without a sintering aid. The tensile strength of Si-C-Al was maintained up to 1600 °C, and 90% of its initial strength was preserved at 1800 °C. The high observed tensile strength retention is believed to be due to its oxygen free composition and its compact structure.

The creep resistance of the ceramic fibers is shown in Fig. 8. It is clear that the creep resistance of the Si-C-Al fibers is much higher than that of either the Si-C-O-Al or Si-C-O fibers. The Si-C-O and the Si-C-O-Al fibers have similar high creep rates above 800 °C; and their creep rate is accelerated above 1000 °C. However, the Si-C-Al fibers began to creep only at 1200 °C. The creep resistance of the three kinds of fibers is closely related to their micro-structural differences. The silicon oxycarbide phase is unstable at high temperature, and is expected to facilitate the diffusion-controlled creep process. On the other hand, some researchers have reported that the carbon phase facilitates grain sliding during creep[25] and subsequently increase the creep rate, although a fundamental understanding of the role of the carbon phase in the creep process remains incomplete.[23] Creep resistance is also related to the SiC fiber crystal grain size. Sacks[26] confirmed that a larger Si C grain size enhances the creep resistance of SiC fibers, which was found to be controlled by the SiC grain size and volume fraction, in combination with secondary phases *etc*.[23] Furthermore, the densification induced by the incorporation of an Al sintering aid during sintering is likely to reduce fiber porosity, and also increase the creep resistance at high temperature as reported.[25]

## Conclusion

High temperature-stable ceramic fibers with the Si-C-Al structure were prepared by sintering (at 1800 °C) Si-C-O-Al ceramic fibers that were manufactured by melt-spinning polyaluminocarbosilane (PACS), air and thermally curing the resulting fibers, followed by a final pyrolysis at 1300 °C. The structural evolution and the associated property changes on moving from Si-C-O-Al to Si-C-Al ceramic fibers during the sintering process were studied in comparison to Si-C-O ceramic fibers. The dependence of properties on microstructure was clarified. The Si-C-O-Al ceramic fibers have a low creep resistance, due to their high silicon oxycarbide content, poorly organized SiC crystalline grain structure at the nanometer level and high levels of free carbon. In addition, these fibers have high electrical resistivity, and this is also attributed to a high level of silicon oxycarbide units. However, the Si-C-Al ceramic fibers show improved tensile strength retention at high temperature thanks to the densification induced by the Al sintering aid and the lower oxygen content arising from the optimized curing conditions. Furthermore, the Si-C-Al ceramic fibers are strongly resistant to creep due to the silicon oxycarbide free structure, the well-organized and crystallized SiC grains and a lower free carbon content, which is probably also responsible for its low electrical resistivity.

## Acknowledgement

This work was supported by the Chinese Natural Science Fund under grant no. 59972042 and Korea Science and Engineering Foundation (KoSEF) no R01-2000-00332.

## References

1 H. P. Baldus and H. Jansen, *Angew. Chem., Int. Ed.*, 1997, **36**(4), 328–343.
2 J. Lipowitz, in *Carbide, Nitride and Boride Materials Synthesis and Processing*, ed. A. W. Weimer, Chapman & Hall, New York, 1997, pp. 433–455.
3 M. Takeda, *Ceram. Eng. Sci. Proc.*, 1996, **174**(4–5), 35.
4 T. Ishikawa, Y. Kohtoko, K. Kumagawa, T. Yamamura and T. Nagasawa, *Nature*, 1998, **391**(19), 773.
5 T. Ishikawa, S. Kajii, T. Hisayuki, K. Matsunaga, T. Hogami and Y. Kohtoku, *Key Eng. Mater.*, 1999, **15**, 164.
6 T. Ishikawa, S. Kajii, T. Hisayuki and Y. Kohtoku, *Ceram. Eng. Sci. Proc.*, 1998, **19**(3), 283.
7 L. B. Coleman, *Rev. Sci. Instrum.*, 1975, **46**, 1115.
8 A. MadronÃero, A. Hendry and L. Froyen, *Compos. Sci. Technol.*, 1999, **59**, 1613.
9 J. A. Dicarlo, *Compos. Sci. Technol.*, 1994, **51**, 213.
10 H. P. Martin, E. Müller, G. Irmer and F. Babonneau, *J. Eur. Ceram. Soc.*, 1997, **17**, 659.
11 G. Chollon, R. Pailler, R. Naslain, F. Laanani, M. Monthioux and P. Olry, *J. Mater. Sci.*, 1997, **32**, 327.
12 C. Laffon, A. M. Flank, P. Lagarde, M. Laridjani, R. Hagege, P. Olry, J. Cotteret, J. Dixmier, J. L. Miquel, H. Hommel and A. P. Legrand, *J. Mater. Sci.*, 1989, **24**, 1503.
13 J. P. Bezombes, C. Chuit, R. J. P. Corriu and C. Reyé, *J. Mater. Chem.*, 1998, **8**(8), 1749.
14 G. D. Soraru, F. Babonneau and J. D. Mackenzie, *J. Non-Cryst. Solids*, 1998, **106**, 256.
15 N. Suyal, D. Hoebbel, M. Mennig and H. Schmidt, *J. Mater. Chem.*, 1999, **9**, 3061.
16 G. W. Wagner, B. K. Na and M. A. Vannice, *J. Phys. Chem.*, 1989, **93**(13), 5061.
17 R. M. Laine and F. Babonneau, *Chem. Mater.*, 1993, **5**, 260.
18 G. J. Chio, W. Toreki and C. D. Batich, *J. Mater. Sci.*, 2000, **35**, 2421.
19 Z. Chen and L. Zeng, *Mater. Res. Bull.*, 1995, **30**(3), 265.
20 G. G. Shi and I. M. Low, *Mater. Res. Bull.*, 1998, **33**(6), 817.
21 J. H. She and K. Ueno, *Mater. Res. Bull.*, 1999, **34**(10/11), 1629.
22 M. Narisawa, Y. Itoi and K. Okamura, *J. Mater. Sci.*, 1995, **30**(13), 3401.
23 D. W. Johnson, A. G. Evans, R. W. Goettler, M. P. Harmer, J. P. Lipowitz, K. Luthra, P. D. Palmer, K. M. Prewo, R. E. Tressler and D. Wilson, *Ceramic Fibers and Coatings: Advanced Materials for the Twenty-First Century*, Publication NMAB-494, National Academy Press, Washington, DC, 1998, pp. 20–36.
24 G. Chollon, R. Pailler, R. Canet and P. Delhaes, *J. Eur. Ceram. Soc.*, 1998, **18**, 725.
25 N. Hochet, M. H. Berger and A. R. Bunsell, *J. Microsc.*, 1997, **185**(2), 243.
26 M. D. Sacks, *J. Eur. Ceram. Soc.*, 1999, **19**, 2305.